Civil Engineering Infrastructures Journal 2023, 56(1): 79-103
DOI: 10.22059/CEIJ.2022.330808.1793

RESEARCH PAPER

Proposed Methodology and Comprehensive Design Process for Seismic Rehabilitation of Steel Structures with Supplemental Viscous Dampers

Bahmani, M.[1] **and Zahrai, S.M.**[2,3]*

[1] Assistant Professor, Department of Civil Engineering, Abadan Branch, Islamic Azad University, Abadan, Iran.
[2] Professor, School of Civil Engineering, College of Engineering, University of Tehran, Tehran, Iran.
[3] Adjunct Professor, Civil Engineering Department, University of Ottawa, Canada.

Received: 17 Sep. 2021; Revised: 06 Jul. 2022; Accepted: 17 Jul. 2022

ABSTRACT: Several types of steel-framed structures now require seismic retrofitting as a result of changes in their usage or modifications in seismic codes. During the last two decades, viscous dampers have been widely used for seismic rehabilitation of buildings because of their ease of application and significant reductions in structural response. The main objective of this research is to present a new comprehensive design process for seismic rehabilitation with non-linear viscous dampers and to introduce the concept of Optimal Retrofit Level (ORL) to control steel buildings. In this article, the inter-story drift as an important parameter of structural response is employed to estimate the failure cost and determine the limit state. Three-, nine- and twenty-story benchmark buildings are used to evaluate the proposed methodology. These buildings have considerably different dynamic properties. The earthquake records corresponding to three levels of seismic hazard are also applied for time-history analysis in order to investigate the trustworthiness of results obtained for zones with different seismicity. The numerical results indicate that the suggested method is able to drop lifecycle costs and creat an equilibrium between rehabilitation costs and failure costs after seismic rehabilitation.

Keywords: Lifecycle Cost, Optimal Retrofit Level, Seismic Retrofit, Steel Buildings, Viscous Dampers.

1. Introduction

The seismic design of buildings is based on life safety criteria or the collapse limit state, but extensive financial damage from recent earthquakes indicates the insufficiency of these criteria to protect the financial resources invested in construction (Shin and Singh, 2014). The financial consequences of recent earthquakes and the modifications to seismic codes highlight the increasing need for seismic retrofit of structures to improve their performance, conducted in two general methods. One is to increase the cross area of the structural member of the building by adding supports and strengthening the main members from the outside by adding steel sheets, fibre-enhanced polymer sheets or post-tensioning. The alternative is to use passive

* Corresponding author E-mail: mzahrai@ut.ac.ir

or active control methods such as energy dissipating devices, seismic isolation or tuned mass dampers (Guo et al., 2014).

Viscous Dampers (VD) are among energy dissipating devices that are commonly used in structures because of their ease of design, simple application in terms of minimum interference with existing building members and increase in damping without a significant increase in the stiffness or mass of the building. VDs are capable of absorbing large amounts of energy induced from earthquakes with little displacement and can decrease both the displacement and acceleration of a structure simultaneously because they are categorized as velocity-dependent dampers (Dall′ Asta et al., 2016).

Over the last two decades, because of the rewards of VDs for seismic rehabilitation of buildings, there have been numerous researches on their engineering and financial aspects. Overall, these studies could be categorized as follows:

- Design strategies for VDs (Kitayama and Constantinou, 2018; Rashid et al., 2022; Silvestri et al., 2010; Wani et al., 2021).
- Effect of nonlinear behaviour of VDs on reduced response of structures (Chopra and McKenna, 2016; Dall′ Asta et al., 2016; Edip et al., 2020; Golnargesi et al., 2022).
- Comparison of different methods for distributing VDs (Hwang et al., 2013);
- Application of VDs in rehabilitation of existing steel buildings (Guo et al., 2014; Sarkisian et al., 2013);
- Reducing the Life Cycle Cost (LCC) of buildings with supplemental VDs (Banazadeh et al., 2017; Ghasemof et al., 2021; Gidaris and Taflanidis, 2015; Salajegheh and Asadi, 2020; Sarcheshmehpour and Estekanchi, 2021; Shin and Singh, 2014);
- Experimental work for verifying proposed design relations (Seleemah and Constantinou, 1997; Sorace et al., 2016);
- Reliability-based optimal design of VDs (Altieri et al., 2018; Aydin et al., 2019; Dall'Asta et al., 2017);
- VDs configuration (Hwang et al., 2008).

Most recent studies on seismic retrofitting of existing structures using VDs focus separately on either the engineering or financial aspects of the matter, although decision-making on seismic retrofits of structures requires a simultaneous study of the engineering and financial effects of seismic retrofitting using passive control methods.

The objective of this study is to introduce a complete and simple design process for the seismic retrofit of steel frames with Non-Linear Viscous Dampers (NLVD) in which the technical and economic aspects of passive control of buildings are taken into account at the same time. The suggested comprehensive design process is presented as a scientific methodology of determining the retrofitting algorithm using NLVDs for professional design engineers. Note that the main research has been conducted in two companion papers: The first part reflected here presents the innovative methodology and detailed design procedure while the second one shows the application of this design process in existing steel buildings recently published elsewhere (Bahmani and Zahrai, 2018).

Compared to design procedures presented in other articles and codes, the proposed comprehensive design procedure has the following advantages: 1) The engineering and economic aspects of design of buildings equipped with VD are evaluated simultaneously; 2) The optimal retrofit level (ORL) is determined more easily and simply using the proposed formula and it is not required to apply optimization algorithms; 3) The design procedure of dampers is a simple and accurate approach and just the natural period of building and mass of each floor are used to specify the characteristics of VDs; 4) The results of comprehensive design procedure have acceptable accuracy for buildings where the distribution of mass and stiffness is not uniform over all floors.

2. Fundamentals of NLVD

This paper will focus on the retrofitting of benchmark building with added VDs. The effect of the added VDs to a benchmark building in resisting seismic force can be clearly explained from energy consideration. The event of a building responding to an earthquake ground motion is described using an energy concept in the follows.

Eq. (1) shows the supplementary force of NLVDs which represents a nonlinear force-velocity relation.

$$F_d = C|\dot{u}|^{\alpha}\, sgn(\dot{u}) \tag{1}$$

where C: is the VD damping coefficient, α: shows the velocity exponent for VD, $\dot{\boldsymbol{u}}$: represents the relative velocity between the two ends of VD, and sgn ( ): represents the sign function.

2.1. Supplemental Damping Ratio (DR) Provided by LVDs

The formulation of supplemental DR using LVDs is provided in chapter 9 of FEMA 356. The DR (ξ) provided by the LVDs for a single degree-of-freedom (SDOF) system vibrating under a cyclic harmonic load is:

$$\xi = \frac{W_D}{4\pi W_S} \tag{2}$$

where W_D: is the energy dissipated by LVDs and W_S: represents the maximum strain energy of the system. The experimental results show that for an increase in the DR of a multi-degree of freedom (MDOF) structure, the higher modes will be suppressed while the first mode will be dominant. Hence, only the first mode of MDOF structures is considered in simplified design methods. Thus, the energy dissipated by the LVDs and the maximum strain energy of the frame for the first mode are calculated as:

$$W_D = \sum_j W_{Dj} = \sum_j \pi C_j \left(\frac{2\pi}{T_m}\right) (u_{roof}\varphi_{mr,j} f_j)^2 \tag{3}$$

$$W_S = \frac{2\pi^2}{T_m^2} \sum_i m_i u_{roof}^2\, \varphi_{mi}^2 \tag{4}$$

All the parameters for Eqs. (3) and (4) are described in the accompanying article (Bahmani and Zahrai, 2018). By applying Eqs. (3) and (4) to Eq. (2), the DR provided by LVD in the primary mode of the structure can be obtained as:

$$\xi_m = \frac{T_m \sum_j C_j\, {\varphi^2}_{mr,j} {f_j}^2}{4\pi \sum_i m_i \varphi_{mi}^2} \tag{5}$$

Eq. (5) is derived by assuming that the first mode of response of the structure is dominant (this assumption is true in most structures). This equation can be approximated in the following structures, where the effects of higher modes are also applied.

- Geometrically irregular buildings;
- A building with irregular mass distribution across its plan and height;
- A building with an irregular rigidity distribution across its plan and height;

2.2. Supplemental DR Provided by NLVDs

The energy dissipated by a NLVD for a SDOF system under cyclic harmonic vibration is as follows (Ramirez et al., 2000):

$$W_D = \int F_d du = \int C_N \dot{u}^{\alpha} du = \lambda C_N \left(\frac{2\pi}{T_m}\right)^{\alpha} u_0^{\alpha+1} \tag{6}$$

$$\lambda = 2^{2+\alpha} \frac{\Gamma^2(1+\frac{\alpha}{2})}{\Gamma(2+\alpha)} \tag{7}$$

in which F_d: represents the damping force, u: represents the displacement of the SDOF system, u_0: shows displacement amplitude or the maximum value of u, C_N: is the damping coefficient of the NLVDs, α: refers to the velocity exponent for the NLVDs and Γ: is the gamma function. Eq. (6) could be developed for MDOF systems as:

$$W_D = \sum_j W_{D,j} = \sum_j \lambda_j C_{N,j} \left(\frac{2\pi}{T_m}\right)^{\alpha_j} (u_{roof}\varphi_{mr,j} f_j)^{\alpha_j+1} \tag{8}$$

By implementing Eqs. (8) and (4) in Eq. (2), the DR provided by the NLVDs in the primary mode of the building can be considered as (Ramirez et al., 2000):

$$\xi_m = \frac{\sum_j \lambda_j C_{N,j} \left(\frac{2\pi}{T_m}\right)^{\alpha_j - 2} u_{roof}^{\alpha_j-1} \varphi_{mr,j}^{\alpha_j+1} f_j^{\alpha_j+1}}{2\pi \sum_i m_i \varphi_{mi}^2} \tag{9}$$

$$\lambda_j = 2^{\alpha_j+2} \frac{\Gamma^2(1+\frac{\alpha_j}{2})}{\Gamma(2+\alpha_j)} \tag{10}$$

in which $C_{N,j}$: is the damping coefficient for the j^{th} NLVD and α_j: refers to the velocity of the j^{th} NLVD.

2.3. Configurations of VDs

As shown in Figure 1, VDs can be installed in four various methods, of which the diagonal and chevron types are very common in practice.

3. Comprehensive Design Procedure

A comparison of the proposed comprehensive design procedure and those published in the literature discloses the relative innovation and straightforwardness of the proposed method given the following features:

- In the suggested comprehensive design procedure, the ORL is determined only by the results of Time-History Analysis (THA) without complicated computations;
- The performance levels, unlike other complex procedures, are explained using the damage states for simplicity;
- The building LCC is estimated for pre-retrofit and post-retrofit conditions using the results of steps two and eight of the technical section of the detailed design process;
- Unlike other studies where the ORL is specified through fragility analysis, the ORL is determined using the simple and clear formula proposed in this study;
- The shear strain energy method is used for the distribution of the damping coefficient. In this method, higher damping coefficient are assigned to floors with more strain energy. Therefore, the viscous dampers contribute to the reduction of the seismic response of the building more effectively.

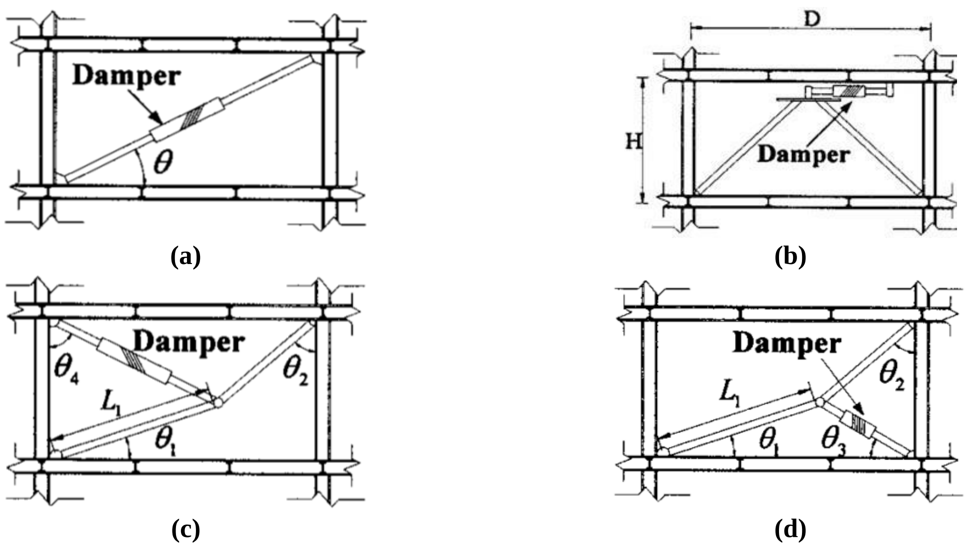

Fig. 1. Installation schemes of viscous dampers: a) Diagonal brace; b) Chevron; c) Upper toggle brace; and d) Lower toggle brace

3.1. Engineering Aspect of Comprehensive Design Procedure

As illustrated in Figure 2, the suggested design process consists of two sections: 1) the design of the NLVDs; and 2) the economic evaluation of the NLVD obtained from Section 1. The Engineering aspect of design process is composed of the following eight steps.

Step E1: Choosing Earthquake Records

Due to the simplicity of implementation, the common approach for seismic analysis of structures is to use the design code spectrum response; however, when a more accurate design is required, it is better to use real earthquake records. In order to assess the suggested comprehensive design process using benchmark structures, two far-field records and two near-field records from Ohtori et al. (2004). A detailed description of the earthquake records is available in Ohtori et al. (2004).

Step E2: FE Model Preparation for Building Without Dampers to Perform THA

Before retrofitting existing structures, for the purpose of evaluate the seismic performance of the bare frame, there is a requirement to build a Finite Element (FE) model and investigate the seismic behaviour of the structure using a FE program. In other words, the prerequisite to any retrofitting plan is to evaluate the existing seismic performance of the building.

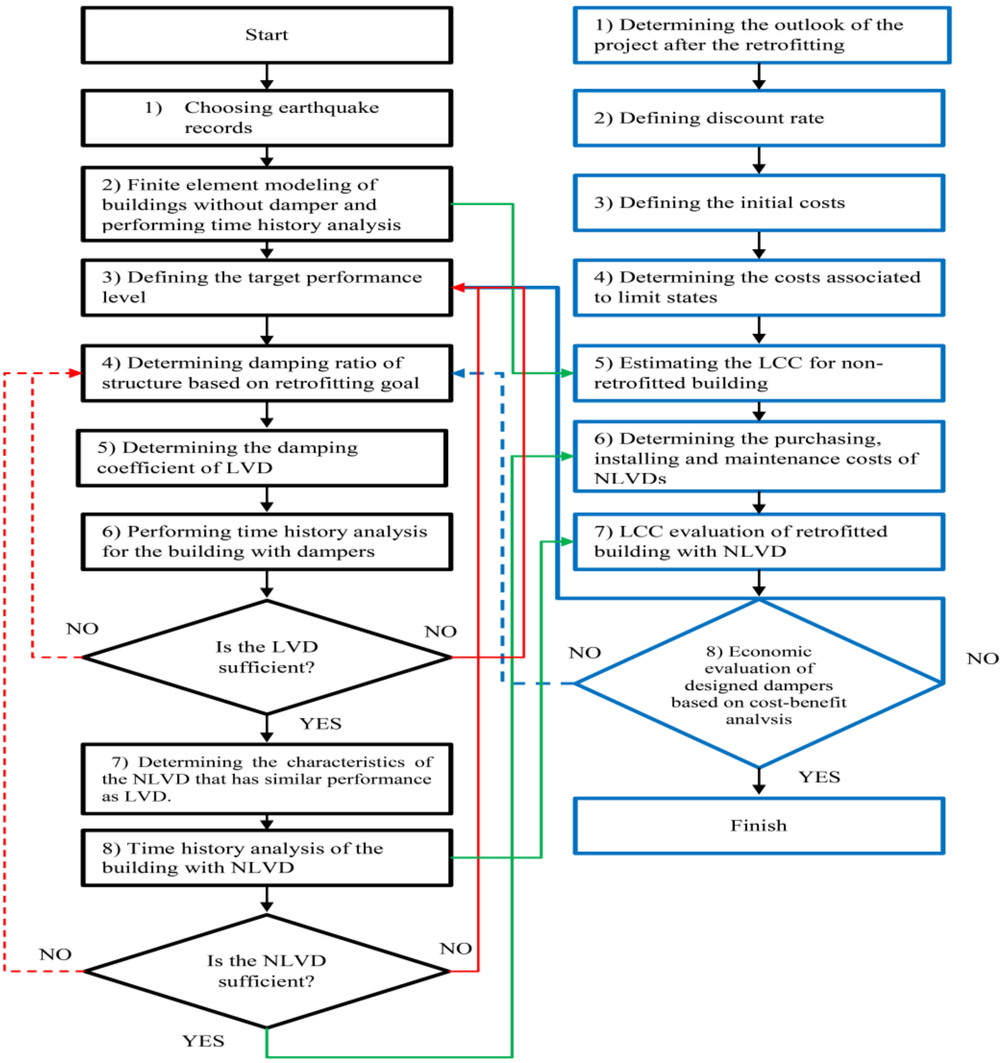

Fig. 2. The proposed comprehensive design procedure in this research for seismic retrofit of existing steel buildings with NLVDs

Step E3: Determining the Retrofitting Target

The upgrade target is based on customer requirements and seismic necessities provided by the design codes. To express performance levels of the structure, such as those shown in Table 1, the limit states presented by FEMA 227 are used in this study. Table 1 shows the maximum Inter-Story Drift (ISD) ratio, an essential parameter of building response that is an indicator of the performance level of the building. Immediate occupancy is the state at which the ISD ratio (Δ) for all buildings is less than 0.7. This is $\Delta \leq 2.5$ for the life safety state and $\Delta \leq 5$ for the collapse prevention state.

Step E4: Determine the Structural DR According to the Rehabilitation Target

Several researchers have provided relations (in engineering accuracy accepted zones) for the DR of dynamic systems (ξ) and its associated seismic response reduction coefficient ($\eta(\xi)$). The effect of ξ on the seismic response of a building is not totally similar at a constant acceleration, velocity or displacement zone, but it can be applied for a period range of typical buildings with acceptable accuracy. In this study, $\eta(\xi)$ of a building ($\eta_\Delta(\xi)$) is the result of the maximum ISD of that building retrofitted with NLVDs divided by the ISD of the building without dampers (inherent damping of $\xi = 0.05$). Here, the equation suggested by (Bommer et al., 2000) is used for defining the relation between the ξ of the structure after rehabilitation and the related reduction of the seismic response.

$$\eta_\Delta(\xi) = \frac{\Delta m_{max}}{\Delta_{max}} \quad (11)$$

$$\eta = \sqrt{\frac{10}{5 + \xi + \xi_m}} \quad (12)$$

Step E5: Determination of the LVD Damping Coefficient

Silvestri et al. (2010) suggested a simplified technique based on the uniform distribution of dampers along the height of building. He assumed the stiffness and weight of all stories to be the same. In the current study, using the comparisons by Hwang et al. (2013) of the various techniques of distributing dampers along height of the structure, the floor shear strain energy method is used. The damping distribution at different stories of the structure for the uniform distribution technique is not proportionate to the maximum dissipating force at each story during earthquake. Compared to other methods of damping distribution, this causes a decrease in the dissipation of the induced earthquake energy.

To assign a constant damping coefficient to the building, the effective DR of the building from the story shear strain energy method is more than that from the uniform distribution method. The VDs from the story shear strain energy method could improve the performance compared to those from the uniform distribution method lowering costs and easing application through decreased interference with the existing structure. Therefore, the use of the story shear strain energy method, a non-iterative method of distributing damping in the building, is more reasonable than the use of other methods because a higher damping coefficient is assigned to the stories of the building having higher shear strain energy, increasing the effectiveness of the dampers.

Table 1. Limit state and the corresponding performance levels

Limit state	Damage state	Story drift ratio (%)	Performance levels
1	None	$\Delta < 0.2$	Immediate occupancy
2	Slight	$0.2 < \Delta < 0.4$	
3	Light	$0.4 < \Delta < 0.7$	
4	Moderate	$0.7 < \Delta < 1.5$	Life safety
5	Heavy	$1.5 < \Delta < 2.5$	
6	Major	$2.5 < \Delta < 5.0$	Collapse prevention
7	Destroyed	$5.0 < \Delta$	

For shear buildings, the strain energy of the floor is proportional to $S_j\varphi_{mj}$; therefore, the damping coefficient at each level can be calculated as:

$$C_j = qS_j\varphi_{mj} \tag{13}$$

in which q: is the proportionality constant and $S_j = \sum_{i=j}^{roof} m_i\varphi_i$. The damping coefficient of the entire structure can be considered as:

$$\sum_i C_i = q\sum_i \varphi_{mi}S_i \tag{14}$$

Using Eqs. (13) and (14), the damping coefficient of each level can be obtained as:

$$C_j = \frac{\varphi_{mj}S_j}{\sum_i \varphi_{mi}S_i}\sum_i C_i \tag{15}$$

Placing Eq. (15) into Eq. (5) produces:

$$\xi_m = \frac{T_m\sum_j[\varphi_{mj}S_j(\sum_i C_i)(f_j\varphi_{mj})^2]}{4\pi(\sum_i m_i\varphi_i^2)(\sum_i \varphi_{mi}S_i)} \tag{16}$$

The damping coefficient of entire structure becomes:

$$\sum_i C_i = \frac{4\pi\xi_m(\sum_i m_i\varphi_i^2)(\sum_i \varphi_{mi}S_i)}{T_m\sum_i[\varphi_{mi}S_i(f_i\varphi_{mi})^2]} \tag{17}$$

Substituting Eq. (17) into Eq. (15) produces the damping coefficient of each level as:

$$C_j = \frac{4\pi\xi_m\varphi_{mj}S_j(\sum_i m_i\varphi_i^2)}{T_m\sum_i[\varphi_{mi}S_i(f_i\varphi_{mi})^2]} \tag{18}$$

Step E6: THA for Building with LVD

THA of the structure with LVDs is carried out using the earthquake records outlined in Step E1. The reason of this analysis is to validate the damping introduced to the structure by the LVDs and compare it to the target DR in Step E4 or, in other words, to calibrate the damping coefficient of LVD to achieve the target performance level as defined in Step E3. When comparing the structural performance of a bare frame and one equipped with dampers, ISD can be used as the effective parameter of structural response. If there is a considerable difference between the initial targets and the level of improvement in the structural behaviour or the DR, Step E4 or E3 should be revised.

Step E7: Determining the Characteristics of NLVDs to Provide Performance Similar to LVDs

The purpose of this step is to determine the features of NLVDs to provide performance similar to that of LVDs under the similar seismic excitation. To specify the damping coefficient of NLVDs using the energy approach, the average energy dissipated by the NLVD and LVD in a SDOF system subjected to all cycles of harmonic vibration is assumed to be equal:

$$\frac{1}{u_0}\int_0^{u_0} W_{DN}du = \frac{1}{u_0}\int_0^{u_0} W_{DL}du \tag{19}$$

$$\frac{1}{u_0}\int_0^{u_0} \lambda C_N\left(\frac{2\pi}{T_m}\right)^{\alpha} u^{\alpha+1}du = \frac{1}{u_0}\int_0^{u_0} \pi C\left(\frac{2\pi}{T_m}\right)u^2du \tag{20}$$

All the parameters of Eqs. (19) and (20) are introduced in the research of Lin et al. (2008). Unifying Eq. (20) produces the following for SDOF systems:

$$C = \frac{3\lambda C_N\left(\frac{2\pi}{T_m}\right)^{\alpha-1} u_0^{\alpha-1}}{\pi(2+\alpha)} \tag{21}$$

in which C: is the damping coefficient for a NLVD in a SDOF system.

For MDOF systems, $u$should be replaced by $u_{roof}\phi_{mr,j}f_j$ to produce:

$$C_j = \frac{3\lambda_j C_{N,j}\left(\frac{2\pi}{T_m}\right)^{\alpha_j-1} (u_{roof}\phi_{mr,j}f_j)^{\alpha_j-1}}{\pi(2+\alpha_j)} \tag{22}$$

where C_j: is the damping coefficient for the NLVD on the j^{th}floor of a MDOF system.

The DR given by NLVDs can be determined as the following when Eq. (22) is inserted into Eq. (5):

$$\xi_m = \frac{3\sum_j \frac{\lambda_j C_{N,j}}{(2+\alpha_j)} \left(\frac{2\pi}{T_m}\right)^{\alpha_j-2} u_{roof}^{\alpha_j-1} \varphi_{mr,j}^{\alpha_j+1} f_j^{\alpha_j+1}}{2\pi \sum_i m_i \varphi_{mi}^2} \quad (23)$$

Step E8: THA of Buildings with NLVD

THA is used to investigate the structural behaviour with NLVDs in order to develop a practical design. The goals of THA at this step are:

- To verify the similar energy dissipation for LVDs and NLVDs under the same seismic excitation;
- To assess the structural performance with NLVDs and compare it to the retrofitting target defined in Step E3;
- To assess the damping provided by the NLVDs and compare it to damping target defined in Step E4.

If the performance target of the structure is not met, Steps E3 and E4 should be revised.

3.2. Financial Aspect of Comprehensive Design Procedure

Decision-making about the seismic retrofit of structures requires concurrent study of the technical and economic effects of the retrofit. Therefore, providing a comprehensive design procedure which includes the design of viscous dampers and an economic assessment of the seismic retrofit is necessary. In other studies on the economic evaluation of seismic retrofit of structures using viscous dampers, two goals have been generally pursued: 1) Minimizing the lifecycle cost of a structure without conducting a feasibility study on the seismic retrofit; and 2) application of evolutionary algorithms to find the optimal parameters for viscous dampers and reduce retrofit costs.

In this study, the feasibility of seismic rehabilitation of structures with VDs is initially investigated through cost-benefit analysis (Eq. (37)). If the benefit-cost ratio is greater than 1, the seismic rehabilitation is economically feasible. If it is less than 1, the seismic retrofit is not recommended (the goal of retrofitting should be revised).

A new parameter called the Retrofit Level (RL) is introduced here which depends on the dynamic response of a structure at various levels of retrofitting to determine the ORL. This section addresses the level of retrofitting which should be chosen as the ORL if the benefit-cost ratio is greater than 1. In this study, Eq. (39) can be applied as a tool for decision-making to introduce an ORL where the initial cost of implementation of seismic retrofitting is balanced by a decrease in the costs of structural failure in future earthquakes.

Step F1: Determine the Design Timeline

Typical buildings have a design horizon of between 40 and 60 years. As obtained by Kappos and Dimitrakopoulos (2008), it is determined that increasing the time frame of the design horizon will increase the benefit-cost ratio. In this study, the design horizon is 50 years.

Step F2: Calculation of the Discount Rate

The discount rate converts the cost of future seismic damage to the net present worth. At a constant discount rate β over continuous time t, the discount rate factor can be expressed as:

$$D(t) = \left\{ \lim_{n\to\infty} \left(1 - \frac{\beta}{n}\right)^n \right\}^t = e^{-\beta t} \quad (24)$$

Step F3: Initial Cost Estimation

The initial costs of a building consist of the material, manufacturing and installation costs of building elements. For steel structures, this is normally considered proportional to the total weight of all structural elements. It also could be affected by parameters such as the cost of connections or other elements of the structure, which plays a role in its workability (Beheshti and Asadi, 2020; Fragiadakis et al., 2006).

Although there is no need to estimate the initial costs of a steel structure in order to determine the ORL, it is used to estimate the costs of the limit states and failure cost. In this article, the 2016 RS Means Building Construction Costs are used to evaluate the initial costs of the building.

Step F4: Calculating the Costs Correlated with Limit States

The cost of the limit state includes the potential cost of damage caused by probable earthquakes in the building lifecycle. The limit state cost is the sum of the earthquake consequences and includes the cost of fixing the damage induced by the earthquake C_i^{dam}, damage to the contents of the building C_i^{con}, relocation C_i^{relo}, lost rent revenue C_i^{ren}, loss of commercial revenue C_i^{inc}, treatment of minor injuries $C_i^{m,inj}$, treatment of serious injuries $C_i^{s,inj}$, fatalities C_i^{fat} and other direct and indirect financial costs. The cost of the i^{th} limit state could be expressed as:

$$C_i^{LS} = C_i^{dam} + C_i^{con} + C_i^{relo} + C_i^{ren} + C_i^{inc} + C_i^{m,inj} + C_i^{s,inj} + C_i^{fat} \quad (25)$$

The details of cost calculations of each parameter with its basic cost for the Los Angeles area and the references for basic cost calculations are listed in Table 2. The third column in the table lists the basic costs according to the 2016 RSMeans Building Construction Costs, changed to present day costs using the following simple formula:

$$\text{Cost in Year A} = \frac{\text{Index for Year A}}{\text{Index for Year B}} \times \text{Cost in Year B} \quad (26)$$

As mentioned, the maximum ISD expresses seven different limit states as reported in FEMA 227. Table 3 lists the damage factors for the seven limit states and other information required to calculate limit states costs.

Table 2 Limit state costs calculation formulas

Cost category	Calculation formula	Adjusted cost	Unit	Reference
Damage	Replacement cost × floor area × damage factor	349.8	/m^2	Whitney
Loss of contents	Unit contents cost × floor area × damage factor	756.2	/m^2	FEMA 227
Relocation	Unit relocation cost × gross leasable area × restoration time	42.3	/month /m^2	FEMA 178
Rental	Rental × rate gross leasable area × restoration time	15.5	/month /m^2	FEMA 228
Income	Rental rate × gross leasable area × restoration time	218.2	/month /m^2	FEMA 228
Minor injury	Minor injury × cost per person × floor area × occupancy rate × expected minor injury rate	2252	/person	FEMA 228
Serious injury	Serious injury × cost per person × floor area × occupancy rate × expected serious injury rate	22522	/person	FEMA 228
Human fatality	Human fatality × cost per person × floor area × occupancy rate × expected death rate	4110000	/life	FEMA 228

Table 3 Limit states, drift ratios, average damage factors, average loss of function, and percentage of minor and serious injuries and death per person occupancy as per ATC-13 and FEMA227

Limit state	Damage state	Story drift ratio (%)	Damage factor	Loss of function (Days)	Minor injury (%)	Serious injury (%)	Death (%)
1	None	$\Delta < 0.2$	0	0	0	0	0
2	Slight	$0.2 < \Delta < 0.4$	0.005	3.4	0.003	0.0004	0.0001
3	Light	$0.4 < \Delta < 0.7$	0.05	12.08	0.03	0.004	0.001
4	Moderate	$0.7 < \Delta < 1.5$	0.2	44.72	0.3	0.04	0.01
5	Heavy	$1.5 < \Delta < 2.5$	0.45	125.66	3	0.4	0.1
6	Major	$2.5 < \Delta < 5.0$	0.8	235.76	30	4	1
7	Destroyed	$5.0 < \Delta$	1	346.93	40	40	20

Step F5: Calculating LCC of Non-Rehabilitated Structure

The LCC of a structure is the cost necessary to maintain a presently occupied structure (during the life of the structure) in accordance with the design target. The LCC of a non-rehabilitated building includes the initial cost, maintenance costs and failure cost caused by design loads.

The initial cost has been explained in detail in Step F3. The maintenance costs include expenditures made to keep the building operational. The failure costs are the damage to structural and non-structural elements of the building due to a probable earthquake during building lifecycle. The failure costs include indirect costs related to the loss or replacement of goods in the building, loss of rental or commercial income, the treatment cost of minor and severe injuries and fatalities among residents. The failure costs associated with a limit state are equal to the limit state cost multiplied by the probability of the structure being exposed to loading of the limit state. Wen and Kang (2001) ignored maintenance costs because they are insignificant relative to initial and failure costs and introduced the following relationship for the LCC of a structure.

$$LCC_{NR} = C_{IN} + C_{FU_{NR}} \tag{27}$$

in which LCC_{NR}: is the LCC for a non-rehabilitated structure, C_{IN}: is the initial cost and $C_{FU_{NR}}$: is the failure cost for the non-rehabilitated structure. The relationship laid out by Wen and Kang (2001) for determining the failure costs of the non-rehabilitated structure is as follows:

$$C_{FU_{NR}} = \frac{\nu}{\beta}(1 - e^{-\beta t}) \sum_{i=1}^{N} C_i^{LS} P_i^{NR} \tag{28}$$

in which P_i^{NR}: is the possibility of the response of a non-rehabilitated structure being at the i^{th} limit state, C_i^{LS}: represents the costs associated with the i^{th} limit state (see Table 2), *N*: is the number of limit states, *t*: denotes the time of the project outlook, β: denotes the discount rate and ν represents the annual occurrence of substantial earthquakes as modelled by the Poisson distribution function. In this equation, P_i^{NR}: is determined as:

$$P_i^{NR} = P_i^{NR}(\Delta > \Delta_i) - P_{i+1}^{NR}(\Delta > \Delta_{i+1}) \tag{29}$$

$$P_i^{NR}(\Delta > \Delta_i) = (-\frac{1}{t}).\, ln[1 - \bar{P}_i^{NR}(\Delta > \Delta_i)] \tag{30}$$

in which $\bar{P}_i^{NR}(\Delta > \Delta_i)$: is the annual exceedance possibility (AEP) of maximum ISD ratio Δ_i. The AEP for the i^{th} limit state is derived as:

$$\bar{P}_i^{NR}(\Delta > \Delta_i) = \rho e^{-\psi \Delta_i} \tag{31}$$

in which ρ and ψ: are obtained by the best fit to the $\bar{P}_i^{NR} - \Delta_i$ pairs. These pairs correspond to earthquakes with probabilities of 2%, 10%, and 50% over 50 years. THA is used to produce the graphs. To conduct THA, three sets of earthquake records that contain longitudinal and traverse components from the Somerville and Collins (2002) database are used here.

Determination of P_i^{NR} for drift Δ_i^{NR} can be carried out by numerical calculation. After calculating P_i^{NR} for the drift percentage related with each limit state, the failure cost is obtained using the THA carried out in Step E2. As shown in Eq. (27), the LCC for a non-retrofitted structure is the sum of the failure cost from this step and the initial cost from Step F3.

Step F6: Determining the Total Cost of NLVDs

To determine the financial adequacy of the NLVDs in Step E8, the costs related to the parts associated to energy dissipation must be evaluated. This cost includes the purchase of NLVDs, their installation and maintenance to keep them in working order. The purchasing cost is proportional to the capacity and stroke range (Taylor, 1999). The installation cost of the dampers includes the bracing on which they are mounted and labour costs. The maintenance cost includes keeping the damper in performance mode after each earthquake such that performance is not affected. The cost associated with dampers may be gained as:

$$C_D = C_0 + \frac{\nu}{\beta}(1 - e^{-\beta t}) \sum_{j=1}^{N} C_j^m P_j \tag{32}$$

in which C_D: refers to the total cost of protective devices, C_0: denotes the initial cost for protective devices, *N*: is the quantity of dampers, C_j^m: represents the cost for damper maintenance and P_j: is the possibility that the devices may need maintenance because of earthquakes.

Step F7: LCC for Rehabilitated Structure with NLVD

The LCC of a structure with NLVDs involves of the initial and failure costs of a structure that is rehabilitated with NLVDs as follows:

$$LCC_R = C_{IN} + C_{FU_R} \tag{33}$$

in which LCC_R: is the LCC of a rehabilitated building and C_{FU_R}: represents the failure cost for a rehabilitated structure. The difference among Eqs. (33) and (27) is determined by assessing the failure costs. The failure costs for rehabilitated structure are calculated by the results of THA (maximum ISDΔ_i^R) in Step E8 as:

$$C_{FU_R} = \frac{\nu}{\beta}(1 - e^{-\beta t}) \sum_{i=1}^{N} C_i^{LS} P_i^R \tag{34}$$

in which P_i^R: is the possibility of a rehabilitated structural seismic response falling into the i^{th} limit state. Determining P_i^R depends on Step E5, except that the probability of corresponding to Δ_i^R is derived from the THA of a retrofitted building to calculate P_i^R.

Step F8: Economic Assessment of Dampers Designed Based on Cost-Benefit Analysis

The calculations in Steps F5 and F7 are used to calculate the expected annual benefit by reducing the earthquake damage to retrofitted buildings as:

$$B_1 = LCC_{NR} - LCC_R \tag{35}$$

in which B_1: is the annual benefit expected due to a decrease in earthquake damage. In order to economically assess the retrofitting applied, the projected benefit in the project outlook is compared to expenditures for rehabilitation. The projected benefit in the design horizon is:

$$B_t = B_1 \frac{1 - (1+\beta)^{-t}}{\beta} \tag{36}$$

in which B_t: is the expected benefit during the design period. For economic assessment of the applied rehabilitation, one can use B_t/C_D as:

$$\frac{B_t}{C_D} = \frac{B_1 \frac{1 - (1+\beta)^{-t}}{\beta}}{C_0 + \frac{\nu}{\beta}(1 - e^{-\beta t}) \sum_{j=1}^{N} C_j^m P_j} \tag{37}$$

If the projected benefit during the design period is larger than the expenditure on rehabilitation the structure, then $B_t/C_D > 1$ and the rehabilitation applied is economical. Otherwise, revisions in Steps E3 and E4 will be necessary.

4. Determining the ORL

In prior sections, a comprehensive design method including the engineering and financial aspects of seismic rehabilitation of buildings with NLVDs has been presented. In the economic evaluation of retrofitted buildings using cost-benefit analysis, only the criterion of $B_t/C_D > 1$ is considered from a financial perspective and no action is taken to address ORL. As stated, most studies that examine the financial effects of seismic retrofitting of structures are focused on the use of evolutionary algorithms to determine optimum design which require time-consuming calculations and bring new complications into the design process for engineers. In this part, to complete this proposed design procedure, a simple method for determining the ORL of structures is introduced based on the LCC of the structure. The flowchart in Figure 3 depicts the proposed method as a complement to comprehensive design procedure.

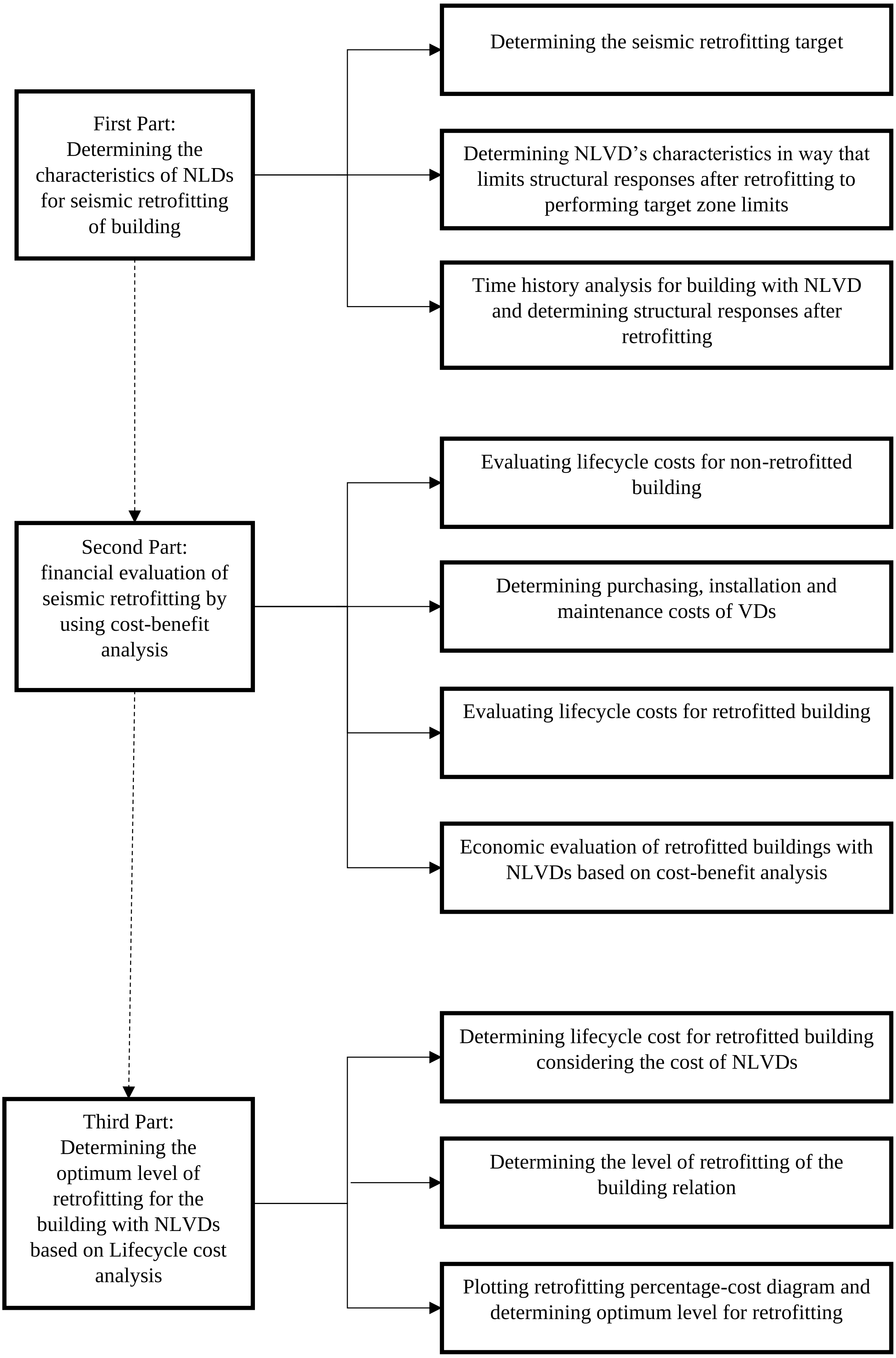

Fig. 3. Proposed method for determining ORL

4.1. Determining the total LCC

In a more general statement than what has been provided in Step F7, the total LCC of the retrofitted building during the design horizon can be calculated as the sum of the initial cost of the building, failure costs due to probable earthquakes in the design horizon and costs associated with the dissipation system. The expected total LCC can be expressed as a function of t and design variable vector X as follows:

$$E[C(t,X)] = C_{IN} + C_D(X) + C_{FU_R}(X) \quad (38)$$

in which $E[C(t,X)]$: is the total LCC over the design horizon. Although the use of NLVDs increases retrofitting costs, a decrease in the likelihood of a failure cost leads to a considerable drop in the costs that are induced by probable earthquakes in the building lifecycle.

4.2. Determining Retrofitting Level Relation

The proposed relation to determine the retrofitting level of the maximum ISD ratio of the stories is presented as:

$$RL = \frac{\Delta}{Before{}^{\Delta^{max_{LS_1}}_{Before}}_{max^{max}_{After}}} \quad (39)$$

in which RL: is the retrofitting level, Δ^{max}_{Before}: denotes the maximum ISD ratio for the state before retrofitting, Δ^{max}_{After}: represents maximum ISD ratio for the state after rehabilitation and Δ_{LS_1}: is the maximum ISD ratio in the first limit state.

The main difference between existing methods for economic assessment of seismic retrofitting and the proposed method is that existing methods seek to minimize the lifecycle cost of a structure at a constant retrofit level, while the RL is employed as an effective variable for the selection of optimal seismic retrofit strategy in the proposed method. In other words, the proposed method uses different *RL* values and the corresponding failure costs to determine ORL.

4.3. Plotting the RL-Cost Diagram and Determining ORL

The ORL is the result of minimizing the LCC of the structure and is the level of seismic retrofitting of a structure for which the total cost of the protective system plus the expected failure cost is minimized. By increasing the RL, the cost of retrofitting will increase, but the failure cost will also drop, because the damage due to probable earthquakes will decrease as well. As shown in Figure 4, the ORL is at the intersection of the diagrams of the damping system costs and expected failure costs due to probable earthquakes over the design horizon. In the design examples, attempts are made to use the proposed relation and design procedure to determine ORL for buildings with different dynamic characteristics under the effect of different earthquakes.

5. Design Examples

Without loss of generality, let’s consider the three benchmark building structures represented in Figures 5 to 7. To assess the suggested comprehensive design process in this research, those three benchmark structures offered by Ohtori et al. (2004) are used. These three, nine, and twenty-story buildings were designed as part of the SAC Steel Project. The reason of selecting these structures for the design examples is to provide a clear basis for assessing the suggested comprehensive design procedure. All three buildings vary considerably in dynamic specifications and lateral strength capacity, thereby providing a broad basis for comparing different structural control strategies. They represent low, medium and high-rise buildings. The structural system for each of the three buildings consists of a perimeter moment-resisting frame and the interior pinned frames using the shear connection. The full description of the structure specifications includes the dimensions, size of members, loading and type of materials used in the study by Ohtori et al. (2004).

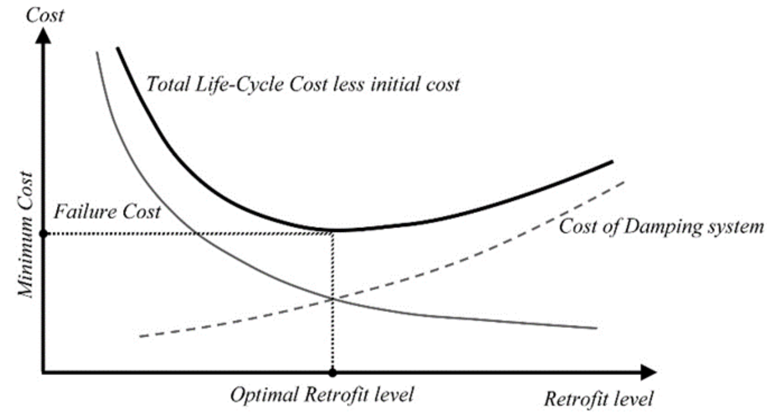

Fig. 4. Retrofitting level-cost diagram

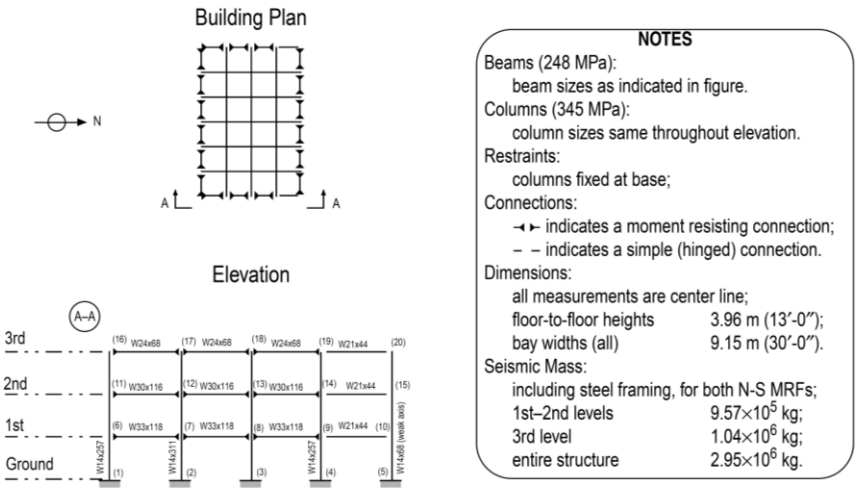

Fig. 5. 3-Story benchmark building N-S MRF (Ohtori et al., 2004)

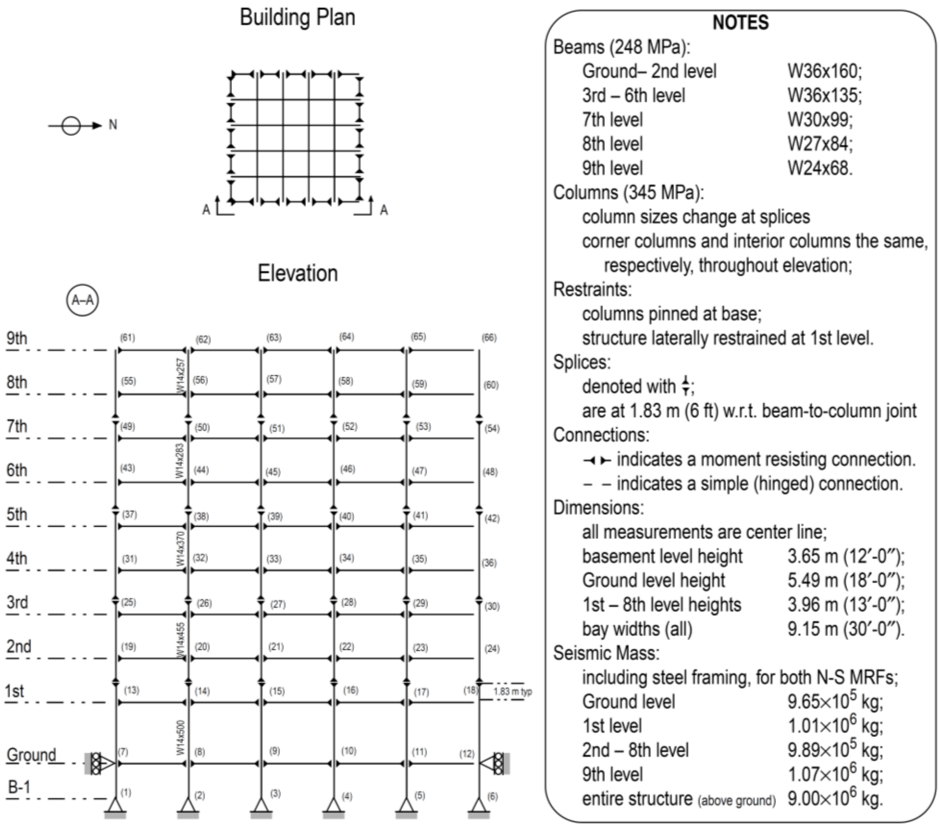

Fig. 6. 9-Story benchmark building N-S MRF (Ohtori et al., 2004)

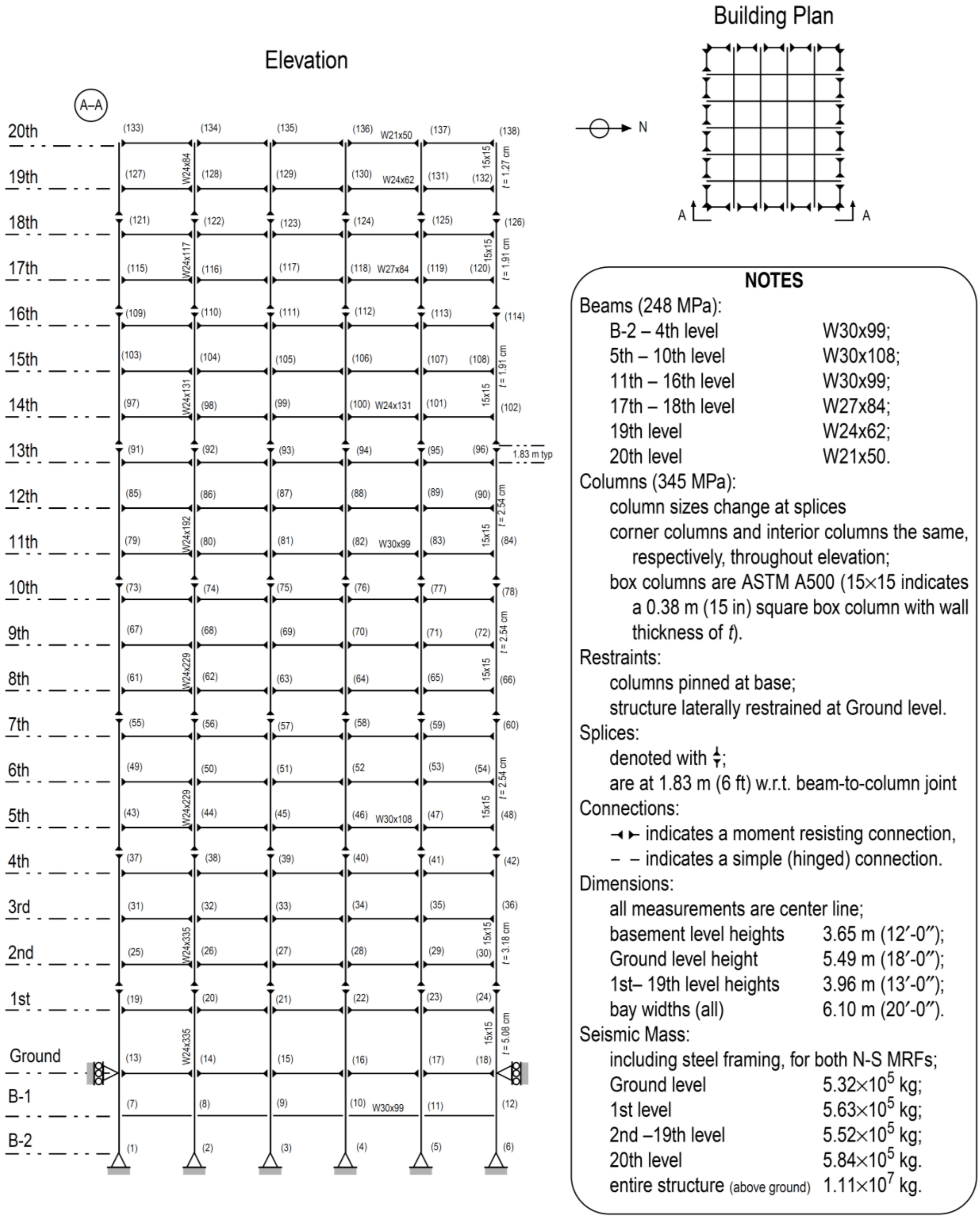

Fig. 7. 20-Story benchmark building N-S MRF (Ohtori et al., 2004)

5.1. Implementing Comprehensive Design Process for Benchmark Structures

In this research, only the important results of implementing the comprehensive design procedure for benchmark structures are presented and interpreted. The complete results of the step-by-step implementation and application of the comprehensive design procedure in the next phase of this research has recently been published in the companion paper (Bahmani and Zahrai, 2018). Based on the results of the THA on buildings without dampers for maximum ISD with different earthquake intensities (0.5, 1 and 1.5), the rehabilitation target is set to a 43% decrease in structural response. Eqs. (17) and (21) can be used to calculate the damping coefficient of LVDs and NLVDs (α = 0.3) as shown in Figure 8 for each story of the benchmark buildings. The lower stories are assigned more damping because the damping distribution in the structure is proportional to the strain energy of the building floors.

As shown in Figure 9, although the seismic retrofitting in all of the benchmark buildings led to the improved seismic performance, the reduction in the ISD for the 9-story structure is higher than that of other buildings.

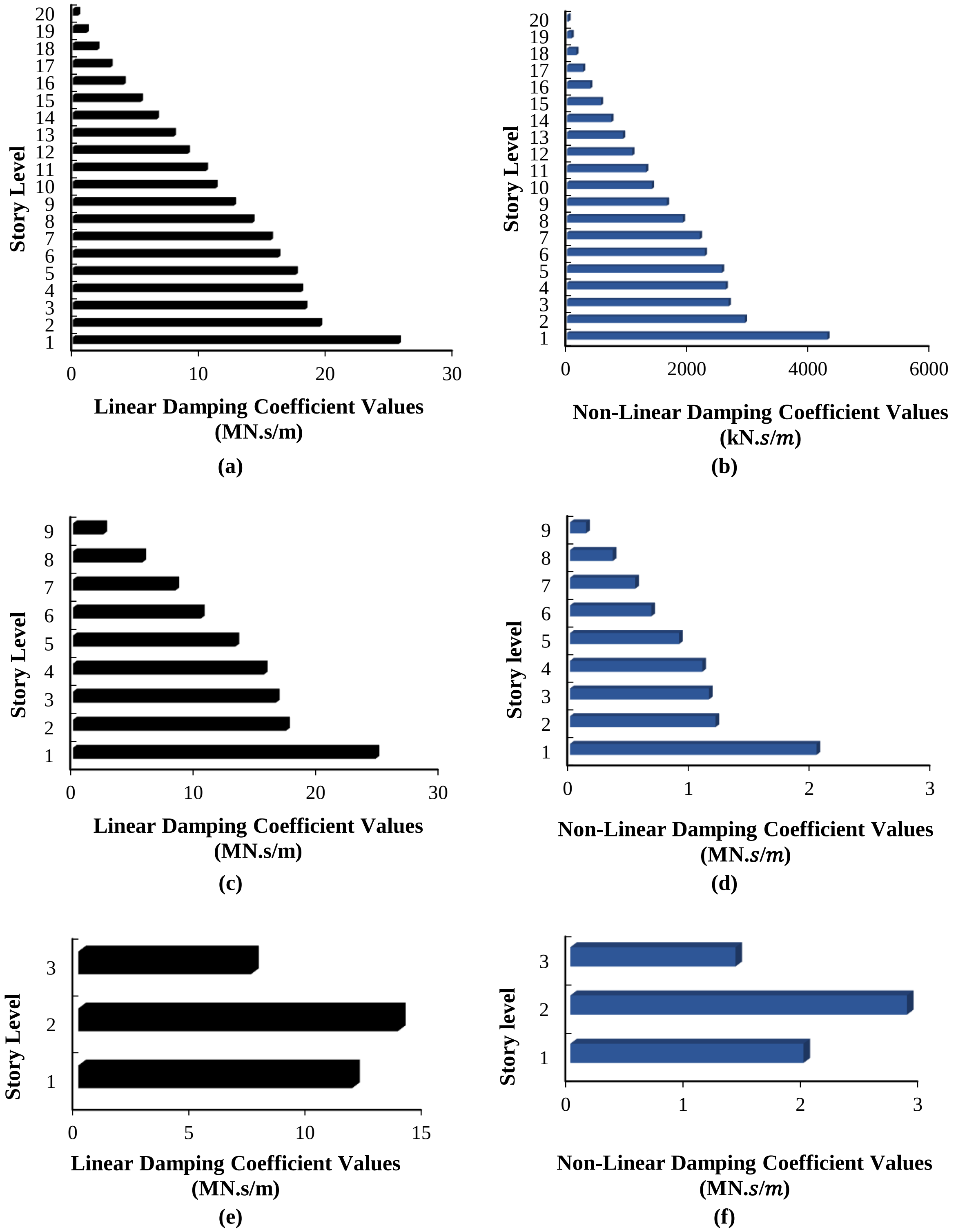

Fig. 8. Damping coefficients of LVDs and NLVDs for benchmark structures: a,b) 20-story; c,d) 9-story; and e,f) 3-story

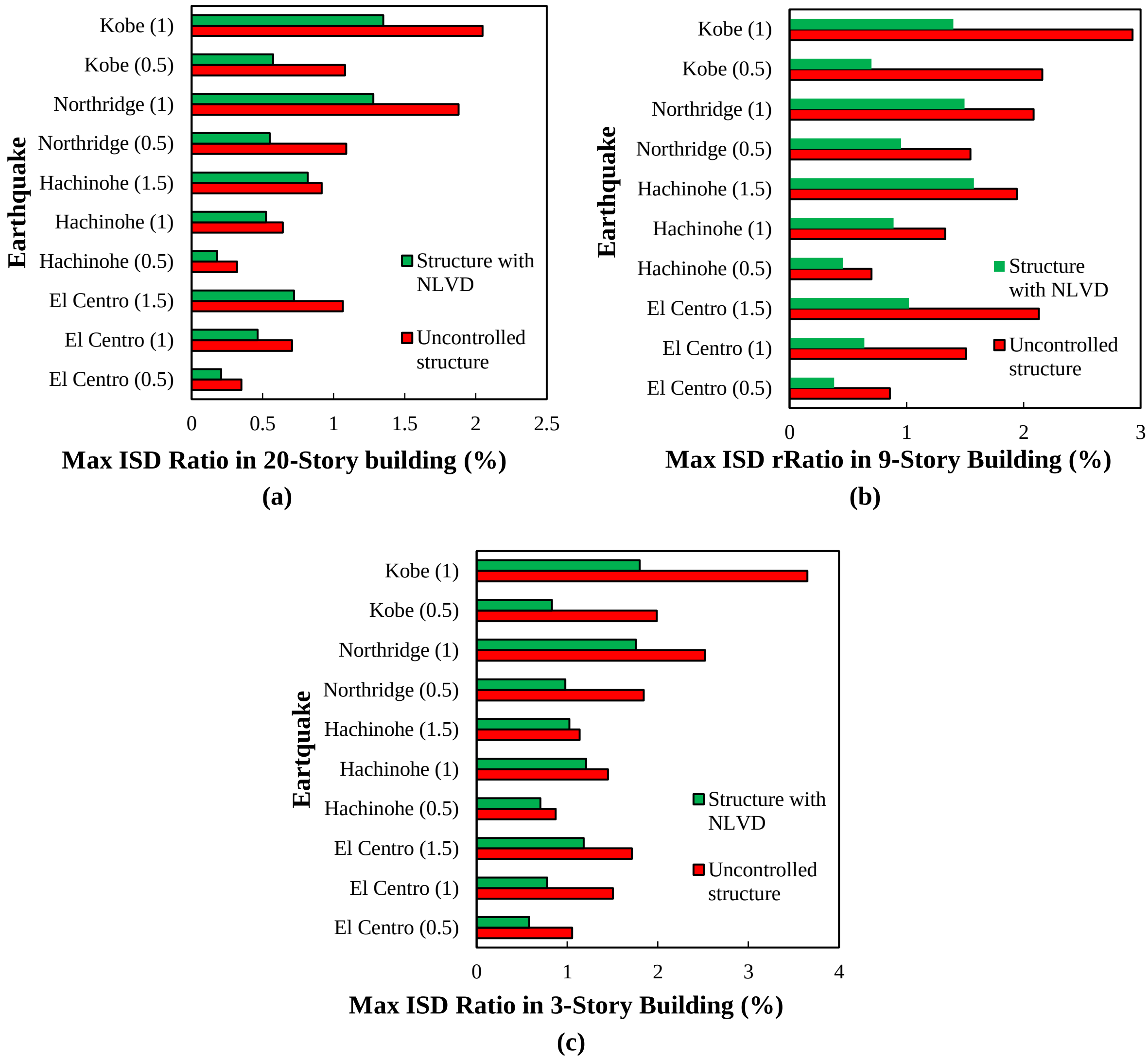

Fig. 9. Maximum ISD ratio in uncontrolled structures and structures with NLVDs: a) 20-story; b) 9-story; and c) 3-story

Figure 10 shows the maximum ISD ratios under each of those four earthquakes with coefficients of 1. As shown here, for each of four earthquake records, the maximum uncontrolled ISD ratios occurred at roof level. This suggests that the comprehensive design procedure is sufficiently capable of controlling the roof response.

Comparison of the results of the comprehensive design process on benchmark structures with NLVDs produced the following points:

- The buildings rehabilitated using the comprehensive design process performed better under low to medium intensity earthquakes than under severe earthquakes.
- Comparison of the results from the THA of the structures retrofitted with NLVDs for 3-, 9- and 20-story building shows that the comprehensive design procedure performed better for medium-rise buildings. In other words, the maximum decrease in seismic response (for an average of ten earthquake records) was in the 9-story building.

Figure 11 depicts the non-linear THA, three pairs of maximum ISD ratios and the AEP for non-retrofitted and retrofitted benchmark buildings. These pairs correspond to earthquakes with probabilities of 2, 10 and 50% over 50 years. As shown in Figure 11, the proposed comprehensive design procedure significantly reduced the ISD ratio of the benchmark buildings at all three levels of earthquake hazard.

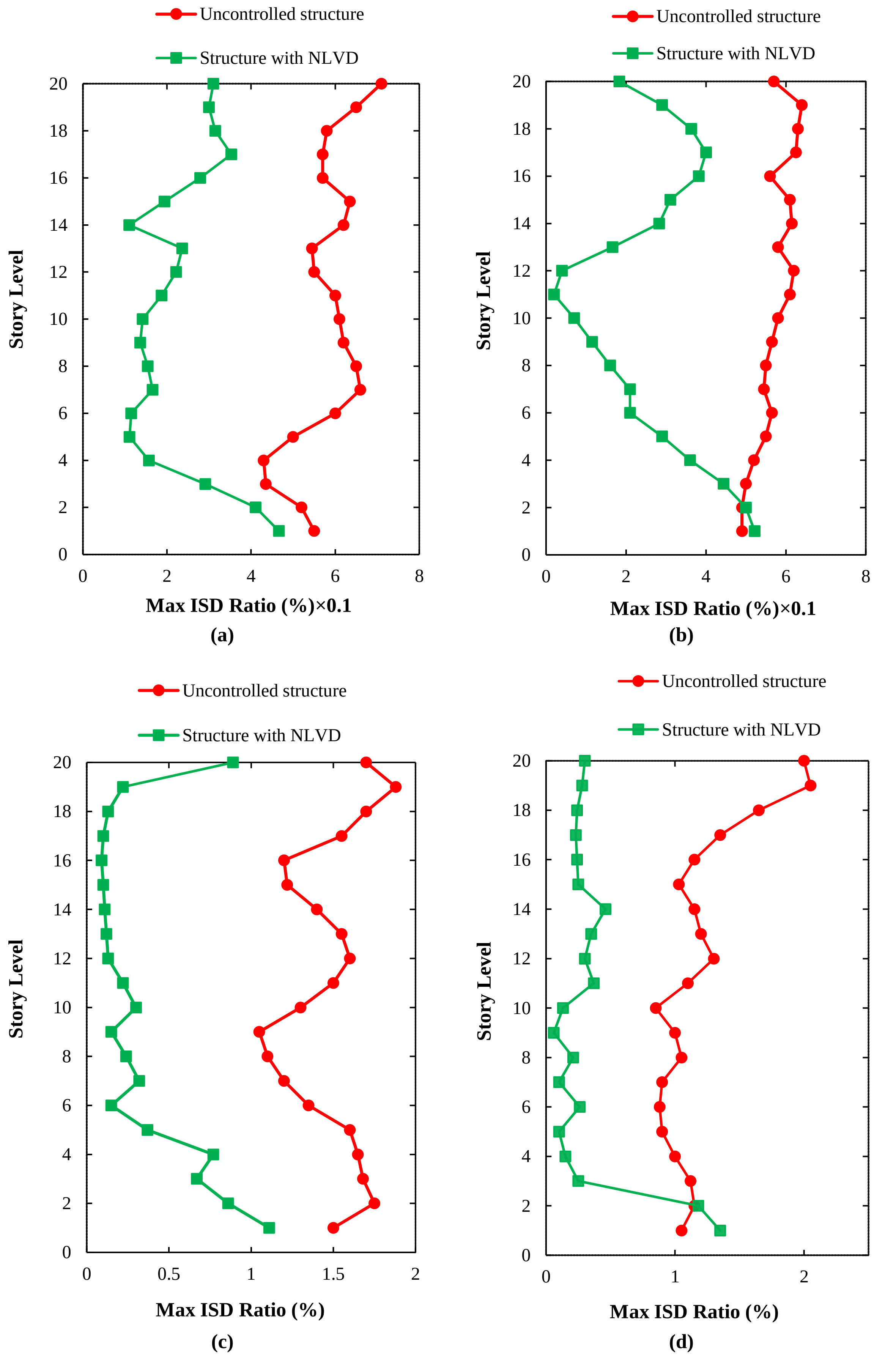

Fig. 10. Maximum ISD ratios for each floor of a 20-story structure subjected to: a) El Centro; b) Hachinohe; c) Northridge; and d) Kobe earthquakes

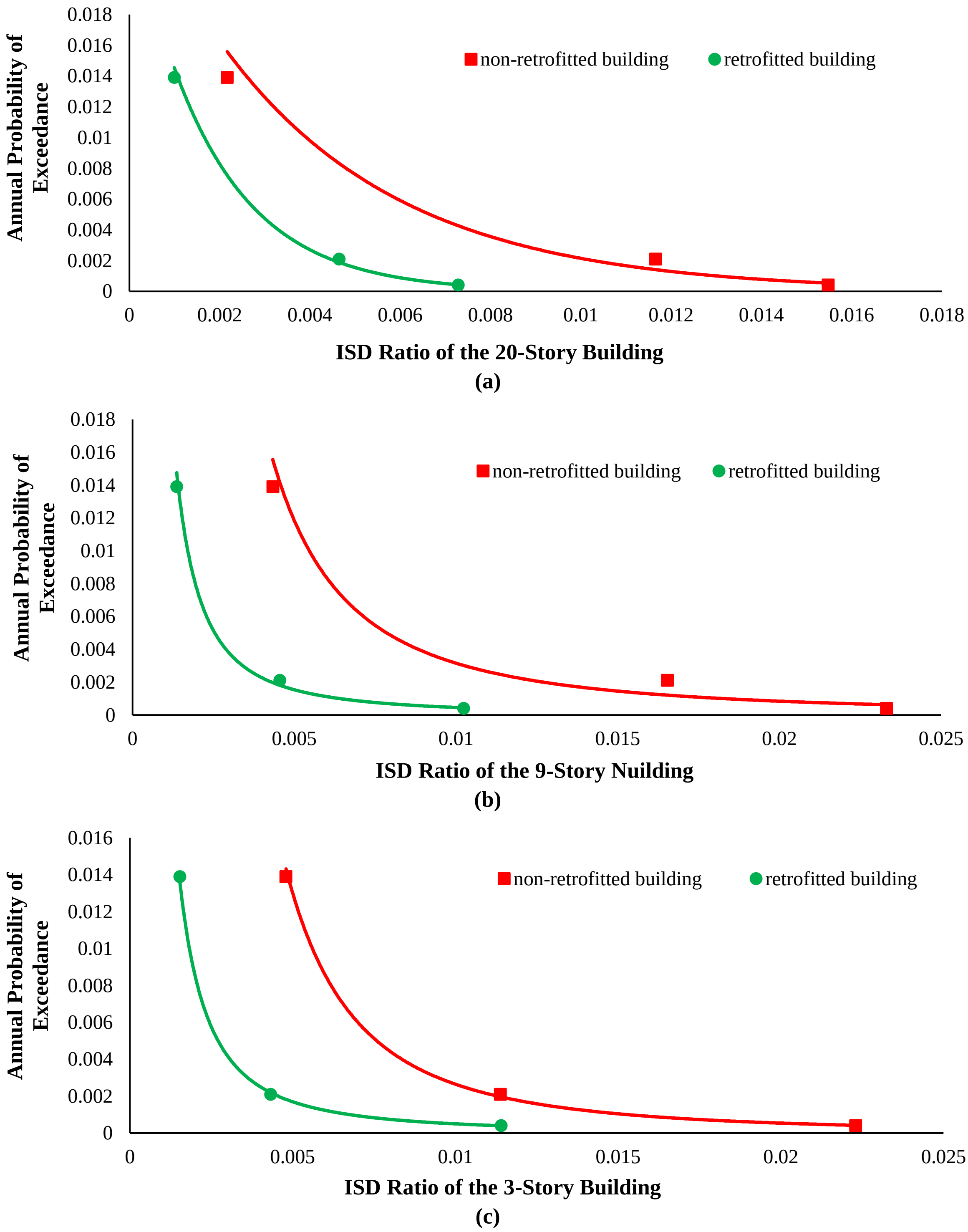

Fig. 11. Comparison of annual probability of exceedance for each damage state for retrofitted and non-retrofitted structures: a) 20-story; b) 9-story; and c) 3-story

The charts plotted for earthquake hazard levels for the probabilities of occurrence of 2%, 10% and 50% over 50 years indicated that the proposed design method significantly could reduce the ISD ratio at all levels of earthquake hazard.

Figure 12 shows that the return periods for 20-, 9- and 3-story buildings were 41, 5 and 16 years, respectively.

To determine the ORL, as mentioned, the failure cost curve is drawn against the cost of the protective system curve. An increase in RL will decrease the ISD and the failure cost. In order to plot the cost curves of the protective system and failure costs, all structures are modelled at three retrofitting levels with NLVDs. Next, for each structure, THA is used with those ten earthquake records defined in Step E1. By determining the maximum ISD for each structure and the maximum auxiliary force of NLVDs at each level, the damping system cost diagram could be plotted for various retrofitting percentages.

Comparison of the retrofitting investment payback period diagrams indicates that the return period is shorter for medium-rise buildings.

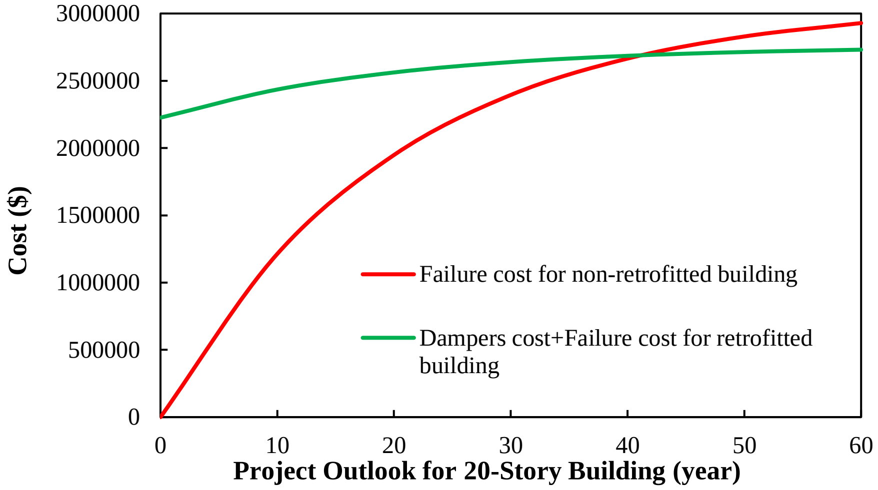

(a)

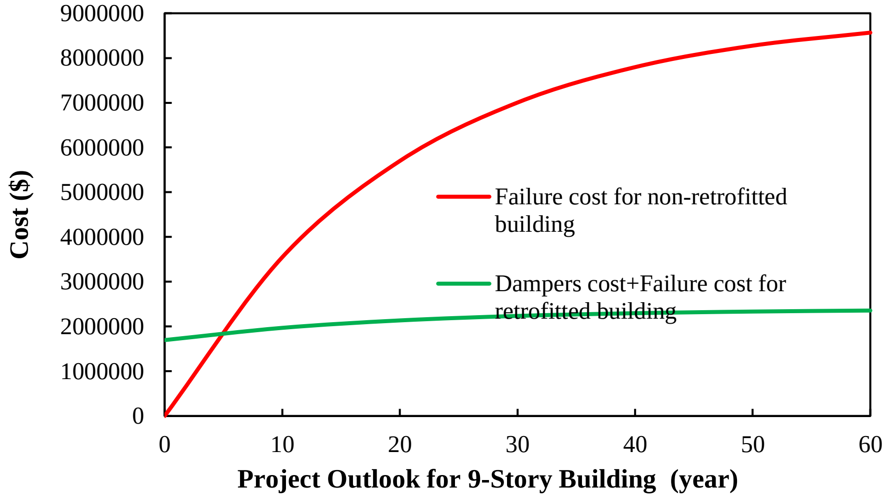

(b)

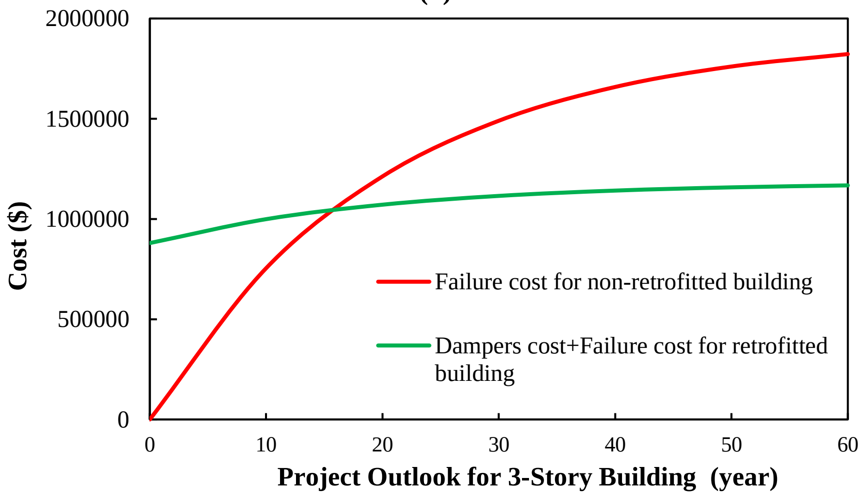

(c)

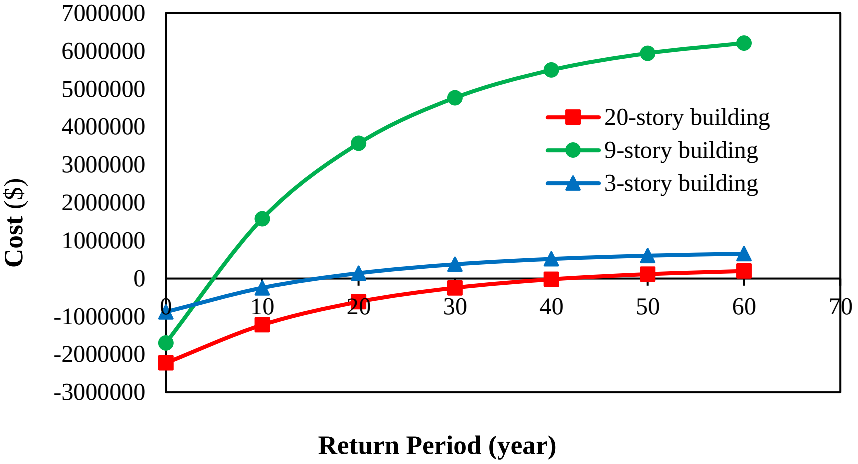

(d)

Fig. 12. Return period for retrofitting investments: a) 20-story; b) 9-story; and c) 3-story

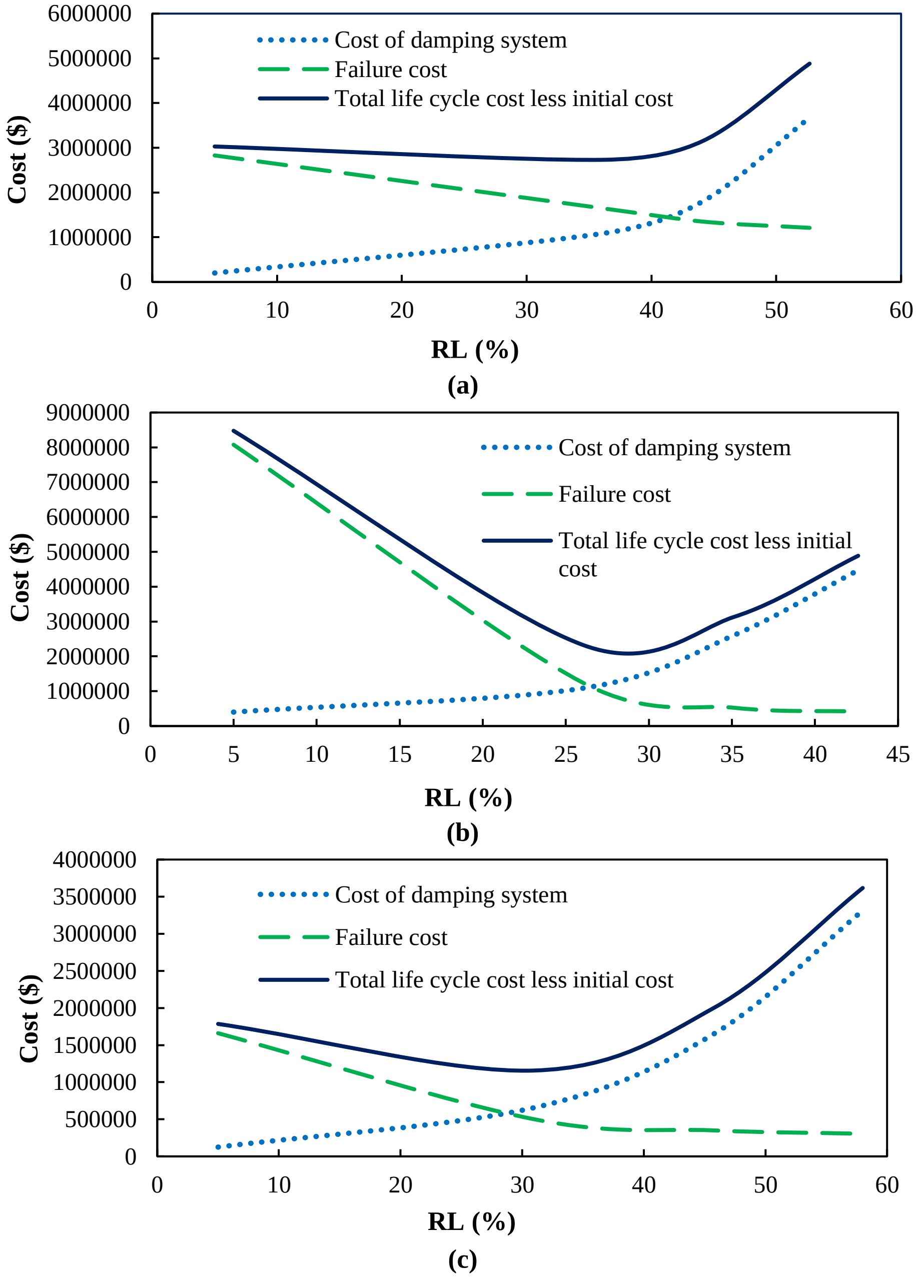

Fig. 13. ORL for: a) 20; b) 9; and c) 3-story buildings

After drawing the failure cost diagrams, each building is subjected to THA under the earthquake records defined in Step F5 and at the end the of Step F7. By determining the failure cost of the RLs, the failure cost diagram for various retrofitting percentages can be drawn. Figure 13 plots the functions of the damping system cost and failure costs for all buildings. As shown, the ORL values for 20-, 9- and 3-story buildings are 40%, 27% and 29%, respectively.

By investigating the curves for determining the ORL, it can be deduced that the ORL in medium-rise structures is lower than that of other structures. In other words, investing less created a greater decrease in the failure costs and the benefit-cost ratio is higher for medium-rise buildings (like the 9-story case) than for the other buildings; hence, implementation of a seismic rehabilitation in these structures has comparative advantages from a financial perspective. Moreover, the benefit-cost ratio increased as the project horizon time increased and the rate of increase in this ratio was rapid for less than 30 years but slowed after 40 years.

5.2. Sensitivity Analysis

The ORL depends on parameters which are often difficult to estimate. The effective parameters for determining ORL are the purchase, installation and maintenance costs of viscous dampers, structural failure costs in future earthquakes for different retrofit levels, design horizons and discount rates. The first two parameters are discussed in Section 5.2 (Figure 13) and sensitivity analysis is conducted here to determine the effect of changes in the design horizon and discount rate on the benefit-cost ratio in this section.

Figure 14 shows how changes in the design horizon and interest rate affect the economic assessment results of seismic retrofitting of the benchmark buildings. As shown, as the design horizon increases for $t < 30$, the benefit-cost ratio increases to a saturation point of about $t = 40$, after which the changes are small. Figure 14 also shows that, as the discount rate increases, the present value of the future benefit and benefit-cost ratio decrease. The high discount rate dramatically reduces the attractiveness of investment in the seismic retrofitting of structures.

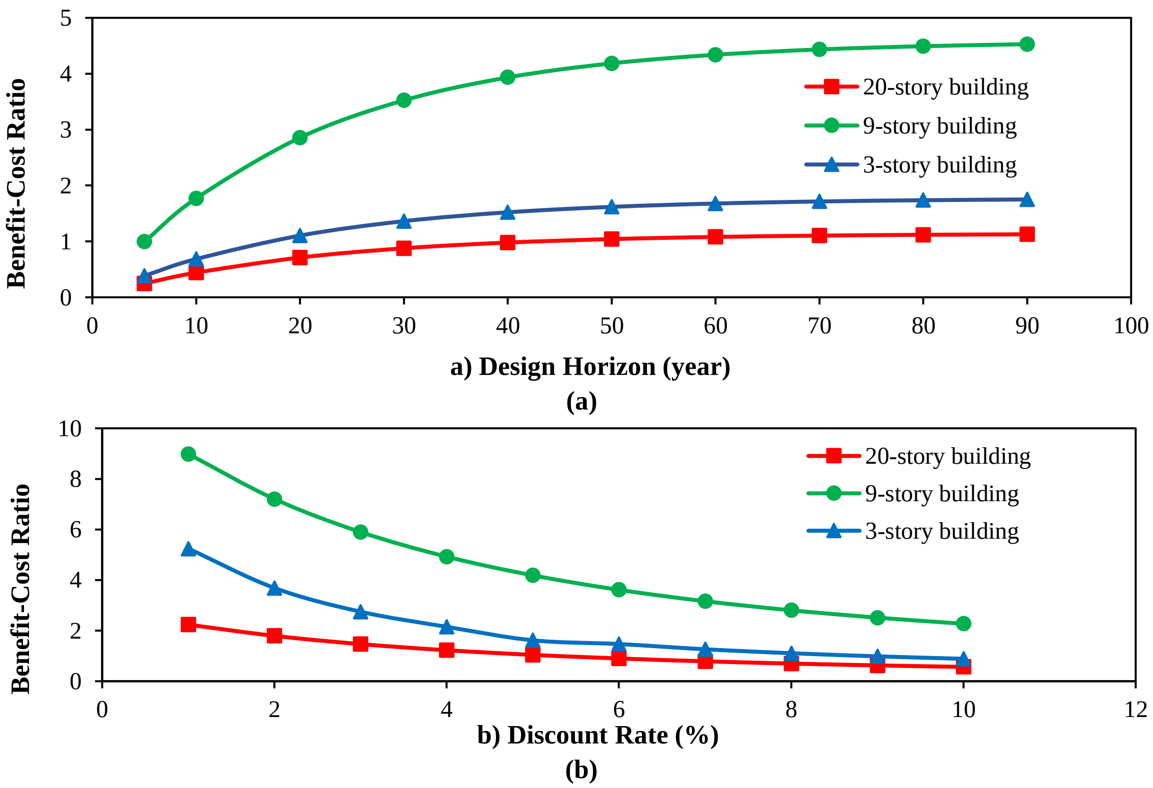

Fig. 14. Effect of: a) design horizon; and b) discount rate on cost-benefit assessment of benchmark structures

As observed in Figure 14 the benefit-cost ratio was sensitive to the discount rate and the high interest rate reduced this ratio dramatically along with the attractiveness of investment for seismic retrofit.

6. Conclusions

The significance of seismic retrofitting and the role of the long-term benefit of the expected failure cost reductions compared to seismic retrofit costs of existing structures are increasingly apparent for structural engineers. The use of NLVDs is an effective method of seismic retrofit of structures. These dampers have become increasingly attractive in recent years due to their comparatively simple design and installation.

Aimed to achieve a scientific design method for professional designer engineers, a comprehensive design process was presented for seismic retrofit of steel buildings in this study. The proposed procedure simultaneously assessed the engineering aspects and economic effects of seismic retrofit. The results of analysis of benchmark buildings revealed that the comprehensive design procedure is accurate enough for buildings with non-uniform distribution of mass and stiffness over the height in spite of other existing design procedures presented in other articles and codes. In the proposed procedure, the ISD ratio was used as the effective parameter of structural response in order to define limit states. The results of analysis of benchmark buildings indicated that the proposed procedure can reduce the response of structures and improve their performance. The numerical results also demonstrated that although the expected failure cost decreases for all structures and earthquakes with various intensities, the suggested design procedure is more influential to improve the performance of middle-rise structures and reduce the failure cost of earthquakes with moderate intensities.

LCC analysis showed that the ORL values for 20-, 9- and 3-story buildings are 40%, 27% and 29%, respectively, and the retrofitting cost return period is shorter for mid-rise buildings. However, the higher benefit-cost ratio in these structures compared to others was a relative financial advantage for seismic retrofitting in medium-rise buildings. Sensitivity analysis showed that the benefit-cost ratio for seismic retrofitting is sensitive to the time horizon of the project and the discount rate. Thus, an increase in the time horizon of the project and reducing the discount rate will increase the attractiveness of investment in seismic retrofitting.

6. References

Altieri, D., Tubaldi, E., De Angelis, M., Patelli, E. and Dall'Asta, A. (2018). "Reliability-based optimal design of nonlinear viscous dampers for the seismic protection of structural systems", *Bulletin of Earthquake Engineering*, 16, 963-982, https://doi.org/10.1007/s10518-017-0233-4.

Aydin, E., Noroozinejad Farsangi, E., Öztürk, B., Bogdanovic, A. and Dutkiewicz, M. (2019). *Improvement of building resilience by viscous dampers*, In: Resilient Structures and Infrastructure, Noroozinejad Farsangi E., Takewaki I., Yang T., Astaneh-Asl A., and Gardoni P., (eds.), Springer, 105-127, https://doi.org/10.1007/978-981-13-7446-3_4.

Bahmani, M. and Zahrai, S. M. (2018). "Application of a comprehensive seismic retrofit procedure for steel buildings using nonlinear viscous dampers", *International Journal of Civil Engineering*, 17(1 August), 1-19, https://doi.org/10.1007/s40999-018-0384-y.

Banazadeh, M., Gholhaki, M. and Parvini Sani, H. (2017). "Cost-benefit analysis of seismic-isolated structures with viscous damper based on loss estimation", *Structure and Infrastructure Engineering*, 13(8), 1045-1055, https://doi.org/10.1080/15732479.2016.1236131.

Beheshti, M. and Asadi, P. (2020). "Optimal seismic retrofit of fractional viscoelastic dampers for minimum life-cycle cost of retrofitted steel frames. *Structural and Multidisciplinary Optimization*, 61(5), 2021-2035, https://doi.org/10.1007/s00158-019-02454-w.

Bommer, J.J., Elnashai, A.S, and Weir, A.G. (2000). "Compatible acceleration and displacement spectra for seismic design codes", *Proceedings of the 12th World Conference on Earthquake Engineering*, Auckland, New Zealand.

Chopra, A. K. and McKenna, F. (2016). "Modeling viscous damping in nonlinear response history analysis of buildings for earthquake excitation", *Earthquake Engineering and Structural Dynamics*, 45(2), 193-211, https://doi.org/10.1002/eqe.2622.

Dall'Asta, A., Scozzese, F., Ragni, L. and Tubaldi, E. (2017). "Effect of the damper property variability on the seismic reliability of linear systems equipped with viscous dampers", *Bulletin of Earthquake Engineering*, 15(11), 5025-5053, https://doi.org/10.1007/s10518-017-0169-8.

Dall′ Asta, A., Tubaldi, E. and Ragni, L. (2016). "Influence of the nonlinear behavior of viscous dampers on the seismic demand hazard of building frames", *Earthquake Engineering and Structural Dynamics,* 45(1), 149-169, https://doi.org/10.1002/eqe.2623.

Edip, K., Bogdanovic, A., Stojmanovska, M., Poposka, A. and Farsangi, E.N. (2020). "A new approach in simulation of soil-structure interaction problems including damper effects", *International Journal of Earthquake and Impact Engineering*, 3(1), 1-14, https://doi.org/10.1504/IJEIE.2020.105377.

Fragiadakis, M., Lagaros, N. D. and Papadrakakis, M. (2006). "Performance-based multiobjective optimum design of steel structures considering life-cycle cost", *Structural and Multidisciplinary Optimization*, 32(1), 1-11, https://doi.org/10.1007/s00158-006-0009-y.

Ghasemof, A., Mirtaheri, M., Mohammadi, R.K. and Mashayekhi, M.R. (2021). "Multi-objective optimal design of steel MRF buildings based on life-cycle cost using a swift algorithm", *Structures*, 34, 4041-4059, https://doi.org/10.1016/j.istruc.2021.09.088.

Gidaris, I. and Taflanidis, A.A. (2015). "Performance assessment and optimization of fluid viscous dampers through life-cycle cost criteria and comparison to alternative design approaches", *Bulletin of Earthquake Engineering,* 13(4), 1003-1028, https://doi.org/10.1007/s10518-014-9646-5.

Golnargesi, S., Shariatmadar, H. and Golnargesi, B. (2022). "Structural control of building with ATMD through AN-IT2FLC under seismic excitation", *Civil Engineering Infrastructures Journal*, 55(2), 309-331, 10.22059/ceij.2021.325512.1760.

Guo, T., Xu, J., Xu, W. and Di, Z. (2014). "Seismic upgrade of existing buildings with fluid viscous dampers: Design methodologies and case study", *Journal of Performance of Constructed Facilities,* 29(6), 04014175, https://doi.org/10.1061/(ASCE)CF.1943-5509.0000671.

Hwang, J.-S., Huang, Y.-N., Yi, S.-L. and Ho, S.-Y. (2008). "Design formulations for supplemental viscous dampers to building structures", *Journal of Structural engineering,* 134(1), 22-31, https://doi.org/10.1061/(ASCE)0733-9445(2008)134:1(22).

Hwang, J.-S., Lin, W.-C. and Wu, N.-J. (2013). "Comparison of distribution methods for viscous damping coefficients to buildings", *Structure and Infrastructure Engineering,* 9(1), 28-41, https://doi.org/10.1080/15732479.2010.513713.

Kappos, A. J. and Dimitrakopoulos, E. (2008). "Feasibility of pre-earthquake strengthening of buildings based on cost-benefit and life-cycle cost analysis, with the aid of fragility curves", *Natural Hazards,* 45(1), 33-54, https://doi.org/10.1007/s11069-007-9155-9.

Kitayama, S. and Constantinou, M.C. (2018). "Seismic performance of buildings with viscous damping systems designed by the procedures of ASCE/SEI 7-16", *Journal of Structural engineering,* 144(6), 04018050, https://doi.org/10.1061/(ASCE)ST.1943-541X.0002048.

Lin, Y.-Y., Chang, K.-C. and Chen, C.-Y. (2008). Direct displacement-based design for seismic retrofit of existing buildings using nonlinear viscous dampers", *Bulletin of Earthquake Engineering,* 6(3), 535-552, https://doi.org/10.1007/s10518-008-9062-9.

Ohtori, Y., Christenson, R., Spencer Jr, B. and Dyke, S. (2004). "Benchmark control problems for seismically excited nonlinear buildings", *Journal of Engineering Mechanics*, 130(4), 366-385, https://doi.org/10.1061/(ASCE)0733-9399(2004)130:4(366).

Ramirez, O. M., Constantinou, M.C., Kircher, C.A., Whittaker, A., Johnson, M.W., Gomez, J.D. and Chrysostomou, C. (2000). *Development and evaluation of simplified procedures for the analysis and design of buildings with passive energy dissipation systems,* MCEER Reports, State University of New York at Buffalo.

Rashid, Z., Tantray, M. and Noroozinejad Farsangi, E. (2022). "Acceleration response-based adaptive strategy for vibration control and location optimization of magnetorheological dampers in multistoried structures", *Practice Periodical on Structural Design and Construction,* 27(1), 04021065, https://doi.org/10.1061/(ASCE)SC.1943-5576.0000648.

Salajegheh, S. and Asadi, P. (2020). "Life-cycle cost optimization of semiactive magnetorheological dampers for the seismic control of steel frames", *The Structural Design of Tall and Special Buildings,* 29(18), e1807, https://doi.org/10.1002/tal.1807.

Sarcheshmehpour, M. and Estekanchi, H. (2021). "Life cycle cost optimization of earthquake-resistant steel framed tube tall buildings", *Structures*, 30, 585-601, https://doi.org/10.1016/j.istruc.2021.01.038.

Sarkisian, M., Lee, P., Hu, L., Garai, R., Tsui, A. and Reis, E. (2013). "Achieving enhanced seismic design using viscous damping device technologies", *Structures Congress 2013: Bridging Your Passion with Your Profession*, ASCE, 2729-2744, https://doi.org/10.1061/9780784412848.237.

Seleemah, A. and Constantinou, M.C. (1997). *Investigation of seismic response of buildings with linear and nonlinear fluid viscous dampers*, National Center for Earthquake Engineering Research, NCEER Publications.

Shin, H. and Singh, M. (2014). "Minimum failure cost-based energy dissipation system designs for buildings in three seismic regions, Part I: Elements of failure cost analysis", *Engineering Structures,* 74(September), 266-274, https://doi.org/10.1016/j.engstruct.2014.04.054.

Silvestri, S., Gasparini, G. and Trombetti, T. (2010). "A five-step procedure for the dimensioning of viscous dampers to be inserted in building structures", *Journal of Earthquake Engineering*, 14(3), 417-447, https://doi.org/10.1080/13632460903093891.

Somerville, P. and Collins, N. (2002). *Ground motion time histories for the Humboldt Bay Bridge*, Pasadena, CA, URS Corporation.

Sorace, S., Terenzi, G. and Mori, C. (2016). "Passive energy dissipation-based retrofit strategies for R/C frame water towers" *Engineering Structures,* 106(1), 385-398, https://doi.org/10.1016/j.engstruct.2015.10.038.

Taylor, D.P. (1999). "Buildings: Design for damping", *Proceedings of the Boston Society of Civil Engineers, BSCES*, Lecture Series: "Dynamics of Structures", USA.

Wani, Z.R., Tantray, M. and Farsangi, E.N. (2021). "Investigation of proposed integrated control strategies based on performance and positioning of MR dampers on shaking table", *Smart Materials and Structures*, 30(11), 115009, https://doi.org/10.1088/1361-665X/ac26e6.

Wen, Y.-K. and Kang, Y. (2001). "Minimum building life-cycle cost design criteria. I: Methodology", *Journal of Structural Engineering*, 127(3), 330-337, https://doi.org/10.1061/(ASCE)0733-9445(2001)127:3(330).